DOI: 10.1002/cmdc.200600122

Arylthiopyrrole (AThP) Derivatives as Non-Nucleoside HIV-1 Reverse Transcriptase Inhibitors: Synthesis, Structure–Activity Relationships, and Docking Studies (Part 2)

Antonio Lavecchia,[b] Roberta Costi,[a] Marino Artico,[a] Gaetano Miele,[a] Ettore Novellino,[b] Alberto Bergamini,[c] Emmanuele Crespan,[d] Giovanni Maga,[d] and Roberto Di Santo*[a]

*Arylthio isopropyl pyridinylmethylpyrrolemethanols (AThPs) have been recently reported as a new class of human immunodeficiency virus type 1 (HIV-1) reverse transcriptase (RT) inhibitors acting at the non-nucleoside binding site (NNBS) of this enzyme. Docking experiments of the potent inhibitors **4k** ($IC_{50}=0.24\ \mu M$, SI = 167) and **5e** ($IC_{50}=0.11\ \mu M$, SI > 1667) of wild-type RT prompted the synthesis and biological evaluation of novel AThP derivatives featuring a number of polar groups in position 3 of the pyrrole ring and larger and more hydrophobic alicyclic substituents in place of the isopropyl group at position 4. Among the compounds synthesized and tested in cell-based assays against HIV-1 infected cells, **19b** was the most active, with $EC_{50}=0.007\ \mu M$, $CC_{50}=114.5\ \mu M$, and SI = 16357. This compound and its precursor **18b** retained interesting activities against clinically relevant drug-resistant RT forms carrying K103N, Y181I, and L100I mutations. Docking calculations of **10**, **14**, **18b**, and **19b** were also performed to investigate their binding mode into the RT NNBS and to rationalize both structure–activity relationship and resistance data.*

Introduction

The introduction of highly active antiretroviral therapy (HAART) involving the use of multidrug combinations has resulted in dramatic declines in death rates from infection by the human immunodeficiency virus type 1 (HIV-1), the causative agent of acquired immunodeficiency syndrome (AIDS). However, the AIDS pandemic remains one of the world's most serious health problems, causing millions of deaths each year, for which no completely successful chemotherapy has been developed so far.[1,2] As such, new anti-HIV agents capable of inhibiting the replication of both wild-type and drug-resistant HIV strains are desperately needed, as is underscored by the rampant spread of the virus throughout Africa. Three different classes of chemotherapeutic agents used in HAART regimens are currently available to block the replication of HIV,[3] namely reverse transcriptase inhibitors (RTIs),[4] protease inhibitors (PIs),[5] and the fusion inhibitor enfuvirtide.[6] The enzyme reverse transcriptase (RT) catalyzes several steps in the replication of HIV, and is an attractive target for anti-AIDS drug development. Two classes of anti-RT agents are currently available: nucleoside reverse transcriptase inhibitors (NRTIs) and non-nucleoside reverse transcriptase inhibitors (NNRTIs).[7] The NRTIs, which include drugs such as AZT (3′-azido-3′-deoxythymidine) and 3TC (lamivudine, 2′,3′-dideoxy-3′-thiacytidine), are converted into their respective triphosphate form by the host and act as dNTP mimics. The NNRTIs, including the "first-generation" drugs such as nevirapine[8] and delavirdine[9] and the "second-generation" inhibitors such as efavirenz[10] (Figure 1), bind to a hydrophobic pocket in the p66 palm subdomain near the polymerase active site.[11] Crystallographic studies have shown that this is the common binding site for many NNRTI classes, and indicate that the mechanism of inhibition takes place by a distortion of the catalytic aspartate residues in the polymerase active site induced by the inhibitor.[12] The therapeutic efficacy of NNRTIs,

[a] *Prof. Dr. R. Costi,[+] Prof. Dr. M. Artico, Dr. G. Miele, Prof. Dr. R. Di Santo*
Istituto Pasteur–Fondazione Cenci Bolognetti
Dipartimento di Studi Farmaceutici
Università degli Studi di Roma "La Sapienza"
P.le A. Moro 5, 00185 Roma (Italy)
Fax: (+39) 6-49913150
E-mail: roberto.disanto@uniroma1.it

[b] *Prof. Dr. A. Lavecchia,[+] Prof. Dr. E. Novellino*
Dipartimento di Chimica Farmaceutica e Tossicologica
Università degli Studi di Napoli "Federico II"
Via D. Montesanto 49, 80131 Napoli (Italy)

[c] *Prof. Dr. A. Bergamini*
Dipartimento di Sanità Pubblica e Biologia Cellulare (DSP&BC)
Università degli Studi di Roma "Tor Vergata"
Via Tor Vergata 135, 00133 Roma (Italy)

[d] *Dr. E. Crespan, Dr. G. Maga*
Istituto di Genetica Molecolare IGM–CNR
Via Abbiategrasso 207, 27100 Pavia (Italy)

[+] *These authors contributed equally to this work.*

Supporting information for this article is available on the WWW under http://www.chemmedchem.org or from the author.

 © 2006 Wiley-VCH Verlag GmbH & Co. KGaA, Weinheim

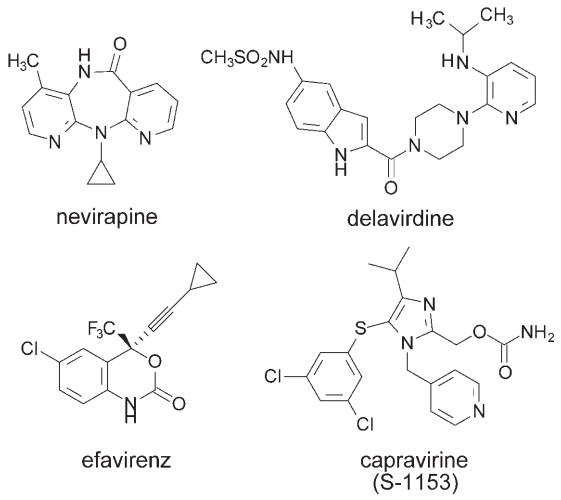

Figure 1. Examples of first- and second-generation NNRTIs.

like other types of anti-AIDS drugs, has been limited by the emergence of drug-resistant viral variants.[13] Therefore, there is an urgent need to develop new drugs with activity against the emerging drug-resistant viruses.

The first generation of NNRTIs is generally very susceptible to the effects of single-point resistance mutations within RT. In contrast, second-generation drugs demonstrate much greater resilience to the presence of such mutations in RT.[14] Recently, capravirine (S-1153, Figure 1) was described[15] and appears to be more resilient than any previously reported compound.[16] S-1153 retains full activity against the most common clinically observed NNRTI resistance mutation, K103N, due to its ability to generate a hydrogen bond grid with the biological target. The molecular portion responsible for this extensive network of H bonds was identified by crystallographic studies as the carbamate group linked at position 2 of the imidazole ring of S-1153.[17] These biological properties guided our efforts toward the synthesis of azole-based S-1153 analogues, with particular regard to pyrrole isosteres.[18] These novel arylthiopyrrole derivatives (AThPs) were designed and synthesized with the aim to obtain new NNRTIs with improved activity and selectivity against HIV-1 RT wild-type and mutant forms with clinically relevant NNRTI-resistant mutations. The AThP derivatives **1**–**4** were proven to be anti-HIV-1 agents targeted against RT (Figure 2). In spite of the fact that the activities of these AThPs are lower than those reported for S-1153, **1** and **2** are less cytotoxic than the reference compound and have selectivity indexes similar to that of S-1153.[18]

After the identification of **1** and **2** as lead compounds related to S-1153,[18] we performed structure–activity relationship (SAR) studies on this novel class of NNRTIs to elucidate the influence of substitution at positions 1 and 5 of the pyrrole ring on biological activity (Part 1 of this series).[19] The pyridinylmethyl group and the 3-methylphenylthio moiety in positions 1 and 5, respectively, gave the highest anti-HIV-1 activities in both enzyme- and cell-based assays.[19] As reported in Part 1 of this series, two active members of the alcohol and carbamate series, namely **4k** and **5e** (following the compound numbering

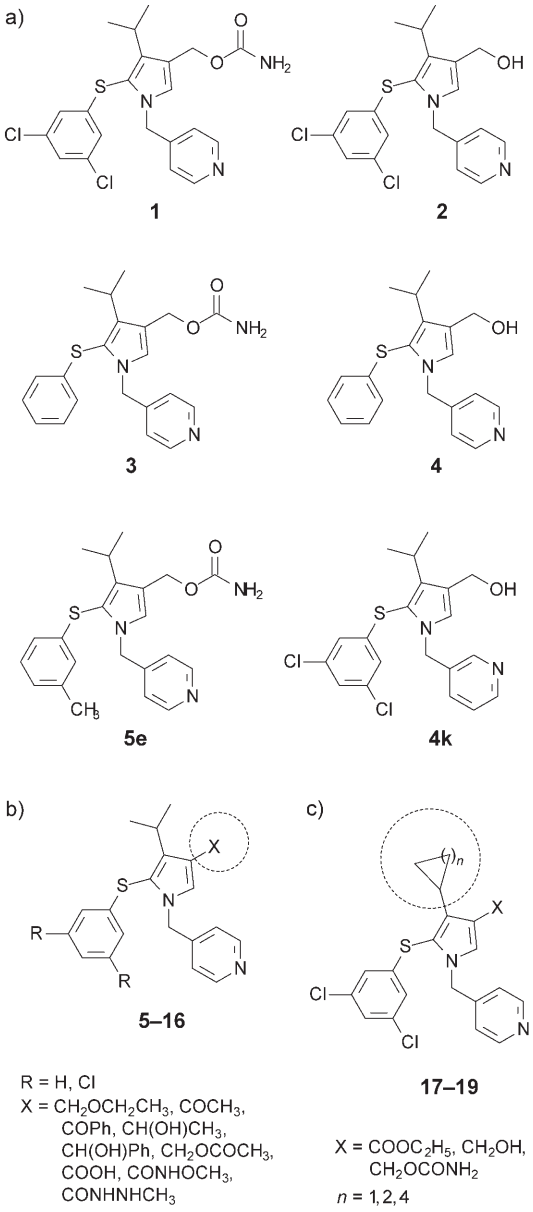

Figure 2. Lead compounds belonging to the AThP class: a) derivatives **4k** and **5e** follow the numbering of Part 1:[19] Planned modifications to the AThP structure: b) polar groups at position 3 of the pyrrole ring and c) substitution of the isopropyl moiety with alicyclic groups.

in Part 1, Figure 2), were docked into the non-nucleoside binding site (NNBS) of HIV-1 RT,[19] allowing some rationalization of both SAR data and the effects of resistance mutations on the binding potencies of the inhibitors. As either a CH_2OH or carbamate group at position 3 of **4k** and **5e** resulted in the formation of H bonds with Lys 101, Lys 103, and the enzyme backbone of Pro 236 (see Figure 3, which depicts the **5e**–RT complex), we planned the synthesis of new AThPs in which the functionality at position 3 is replaced with a number of groups that are potentially able to form H bonds with the biological target (compounds **5**–**16** in Figure 2).

 © 2006 Wiley-VCH Verlag GmbH & Co. KGaA, Weinheim

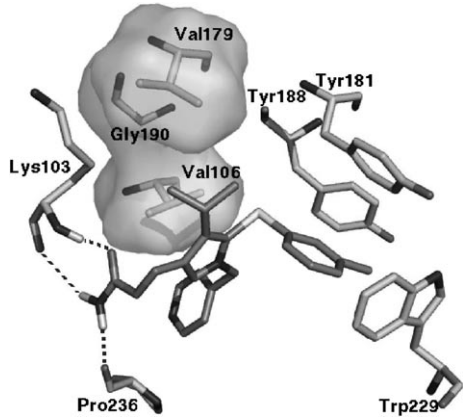

Figure 3. Compound **5e** (of Part 1[19]) docked within the HIV-1 RT NNBS. Only the interacting key residues (including a transparent Connolly surface of Val 106, Gly 190, and Val 179 of the RT binding site) are shown for simplicity. Hydrogen bonds are indicated with dashed lines. Hydrogen atoms are omitted for the sake of clarity, except those involved in H-bond interactions.

Moreover, inspection of the **4k**–RT and **5e**–RT complexes of Part 1 revealed that the isopropyl group at position 4 of the inhibitor pyrrole ring could be replaced by larger and more hydrophobic alicyclic substituents. Such substituents were expected to occupy the NNBS pocket so as to contact the hydrophobic residues Gly 190, Val 179, and Val 106, as shown in Figure 3. Hydrophobicity is a key feature driving the potency of inhibitor binding to the NNBS site, and thus the identification of hydrophobic binding sites is an important consideration in the design of NNRTIs. Accordingly, compounds **17**–**19** (Figure 2) were proposed for synthesis.

Herein we report the design, synthesis, and SAR studies of AThP derivatives **5**–**19** as pyrrole analogues of capravirine which were tested for their ability to block the HIV-1 replication cycle in infected MT-4 cells. Selected compounds were tested in enzyme assays against both wild-type and some mutated rRT forms of clinical interest. Moreover, to elucidate the binding mode of these novel AThP derivatives in the NNBS of HIV-1 RT, compounds **10**, **14**, **18b**, and **19b** were subjected to docking simulations. This allowed rationalization of SAR and drug-resistance data.

Chemistry

The synthesis of compounds **5**–**19** is shown in Schemes 1–4. Derivatives **17**–**19** were prepared starting from the appropriate acrylates **20a**–**c**,[20–22] which underwent cycloaddition of tosylmethyl isocyanide (TosMIC) in the presence of NaH to give pyrroles **21a**–**c**. These compounds were treated with 3,5-dichlorophenylsulfenyl iodide as the electrophile generated in situ with 3,5-dichlorothiophenol, potassium iodide, and iodine to afford the 5-arylthiopyrroles **22a**–**c** that were further alkylated with 4-pyridylmethyl chloride hydrochloride in alkaline medium to furnish **17a**–**c**. Reduction of esters **17a**–**c** with lithium aluminum hydride gave the corresponding alcohols **18a**–**c**, which were carbamoylated in two steps by reaction with trichloroacetyl isocyanate and hydrolysis in alkaline medium to afford carbamates **19a**–**c** (Scheme 1).

A similar synthetic pathway led to compounds **6**–**9**. Pyrroles **24a** and **24b** were obtained by TosMIC annulation with the appropriate enone **23a**[23] and **23b**.[24] Reaction of **24a** and **24b** with 3,5-dichlorothiophenol, KI, and I_2 gave pyrroles **25a** and **25b**, which were alkylated with 4-pyridylmethyl chloride to afford **6** and **7**, respectively. Reduction of the latter compounds with sodium borohydride gave the corresponding alcohols **8** and **9** (Scheme 2).

Derivatives **11**–**16** were synthesized as shown in Scheme 3. The alkaline hydrolysis of esters **26**[18] and **27**[18] led to pyrrole-3-carboxylic acids **11** and **12**, respectively, which were activat-

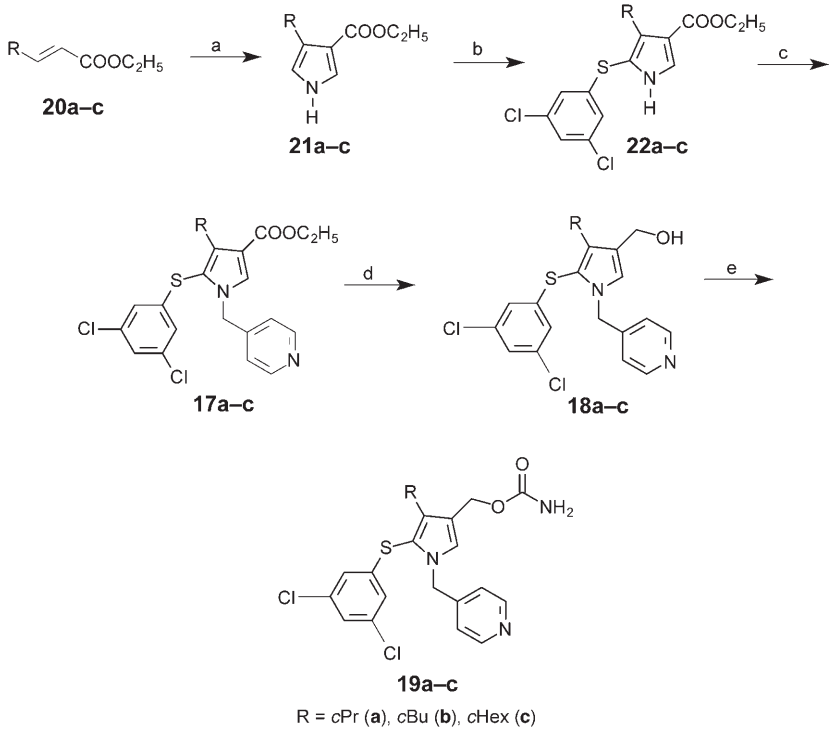

Scheme 1. Synthesis of compounds **17**–**19**: a) TosMIC, NaH, DMSO/Et_2O, RT; b) 3,5-dichlorothiophenol, KI, I_2, EtOH/H_2O, reflux; c) pyridinylmethyl chloride hydrochloride, TBAHS, NaOH (50%), CH_2Cl_2, RT; d) $LiAlH_4$, THF, RT; e) trichloroacetylisocyanate, CH_2Cl_2, RT, 1.5 h; K_2CO_3, MeOH/H_2O, RT, 3.5 h.

 © 2006 Wiley-VCH Verlag GmbH & Co. KGaA, Weinheim

ed with 1-hydroxybenzotriazole (HOBT), *N*-methylmorpholine (NMM), and *N*-(3-dimethylaminopropyl)-*N'*-ethylcarbodiimide hydrochloride (EDCI) and then treated with the proper nucleophile to furnish compounds **13**–**16** (Scheme 3).

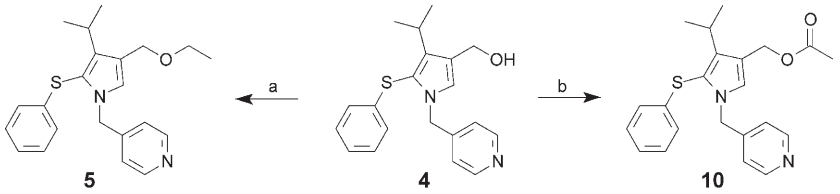

Scheme 4. Synthesis of compounds **5** and **10**: a) HCl, EtOH, RT, 20 min; b) Ac_2O, DMAP, TEA, RT, 20 min.

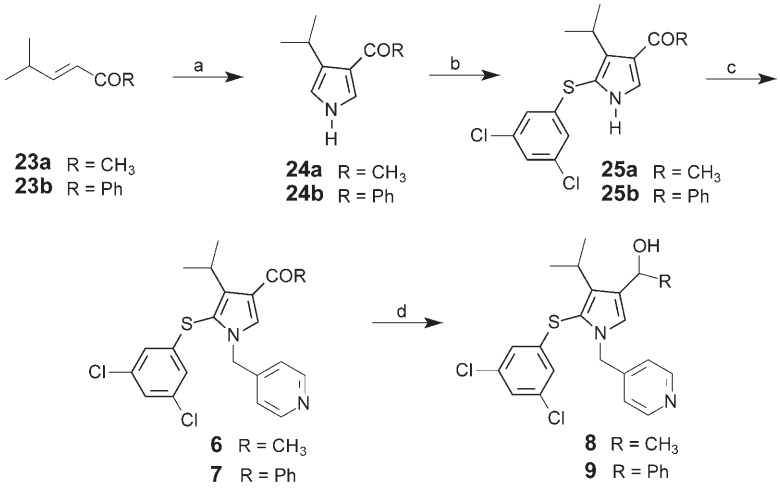

Scheme 2. Synthesis of compounds **6**–**9**: a) TosMIC, NaH, DMSO/Et_2O, RT; b) 3,5-dichlorothiophenol, KI, I_2, EtOH/H_2O, reflux; c) pyridinylmethyl chloride hydrochloride, TBAHS, NaOH (50%), CH_2Cl_2, RT; d) $NaBH_4$, MeOH, RT.

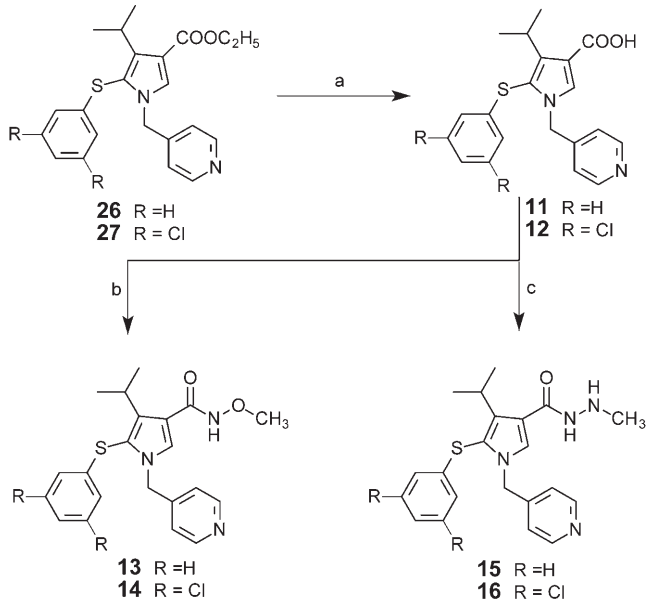

Scheme 3. Synthesis of compounds **11**–**16**: a) NaOH (20%), EtOH, reflux, 2.5 h; b) CH_3ONH_2, HOBT, NMM, EDCI, CH_2Cl_2, RT; c) CH_3NHNH_2, HOBT, NMM, EDCI, CH_2Cl_2, RT.

Finally, the treatment of alcohol **4**[18] with hydrochloric acid in ethanol gave ether **5**, whereas its reaction with Ac_2O in the presence of *N*,*N*-dimethylaminopyridine (DMAP) and Et_3N (TEA) gave the ester **10** (Scheme 4).

Results and Discussion

Anti-HIV-1 cell-based assays and anti-rRT assays

The novel AThP derivatives **5**–**19** were tested for their cytotoxicity and anti-HIV-1 activity in MT-4 cells in comparison with nevirapine,[8] S-1153,[15] and compounds **1**[18] and **2**[18] used as reference drugs. The results, expressed as CC_{50} (50% cytotoxic concentration), EC_{50} (50% HIV-1 replication inhibitory concentration), and SI (selectivity index, given by the CC_{50}/EC_{50} ratio) values are summarized in Table 1. All tested compounds but one were found active against the HIV-1 replication cycle in infected cells. Ten out of the 21 compounds tested showed anti-HIV-1 activity at sub-micromolar concentrations, and generally had low cytotoxicity. Compound **19b** was the most potent AThP derivative of this series, with EC_{50} = 7 nM, CC_{50} = 114.5 μM, and SI = 16357. **19b** was about 35-fold more active than nevirapine and was similar to S-1153 in activity.

The carbamate and the carbinol branch of lead compounds **1**–**4** were replaced with a number of groups capable of forming H bonds. As a rule, the newly synthesized derivatives **5**–**16** were less potent than the reference compounds. In general, the 3,5-dichlorophenylthio derivatives were more potent than their phenylthio counterparts, thus confirming the results previously obtained with carbinols and carbamates **1**–**4**.[18] The most interesting NNRTIs designed in the present work are the acetyloxymethyl derivative **10** and the methyl hydroxamate **14**, which are 17- and 13-fold less potent than compound **2**, respectively.

The introduction of a methyl group or phenyl ring on the carbon atom of the hydroxymethyl group of lead compound **2** led to carbinols **8** and **9**, which were 40–800 times less potent than the reference counterpart. Interestingly, phenyl derivative **9** was 22-fold more potent than compound **8**. This result was confirmed in the ketone series (compare compounds **6** and **7**) and led us to hypothesize that a π-stacking interaction could be ascribed to the phenyl ring in the interaction with the binding site. Finally, ketones **6** and **7** were less potent than the corresponding alcohols **8** and **9**.

Replacement of the isopropyl group at position 4 of the pyrrole ring in **1** and **2** with cyclopropyl, cyclobutyl, or cyclohexyl moieties gave derivatives **18a**–**c** and **19a**–**c**. Among the carbamate series, the cyclobutyl derivative **19b** was more potent than its cyclohexyl counterpart **19c**, and this compound was more active than the cyclopropyl analogue **19a**. Similar results

 © 2006 Wiley-VCH Verlag GmbH & Co. KGaA, Weinheim

Table 1. Cytotoxicity, anti-HIV-1, and anti-rRT activities of AThP derivatives **5–19**.[a]

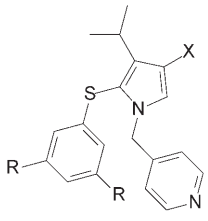

5–16

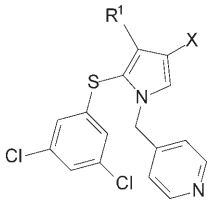

17–19

Compd	X	R	R^1	CC_{50} [μM][b]	EC_{50} [μM][c]	SI[d]	IC_{50} [μM][e]			
							Wild-type	K103N	Y181I	L100I
5	$CH_2OCH_2CH_3$	H		180	7	25.7				
6	$COCH_3$	Cl		>200	29	>6.9				
7	COPh	Cl		45	12	3.8				
8	$CH(OH)CH_3$	Cl		>200	26	>7.7				
9	CH(OH)Ph	Cl		20	1.2	16.7				
10	CH_2OCOCH_3	H		>200	0.5	>400	0.3			
11	COOH	H		190	4.7	40				
12	COOH	Cl		>200	2.1	>95				
13	$CONHOCH_3$	H		>200	1.9	>105				
14	$CONHOCH_3$	Cl		40	0.4	100	1.0			
15	$CONHNHCH_3$	H		>200	>200					
16	$CONHNHCH_3$	Cl		184	4	46				
17a	$COOC_2H_5$		*c*Pr	70	1.5	47				
17b	$COOC_2H_5$		*c*Bu	80	0.3	267	1.04			
17c	$COOC_2H_5$		*c*Hex	95.1	0.64	149	0.61			
18a	CH_2OH		*c*Pr	80	0.2	400	0.43			
18b	CH_2OH		*c*Bu	94.6	0.08	1183	0.08	43.3	10.4	1.16
18c	CH_2OH		*c*Hex	84.0	0.22	382	38.2			
19a	CH_2OCONH_2		*c*Pr	121.7	0.65	187	0.55			
19b	CH_2OCONH_2		*c*Bu	114.5	0.007	16357	0.04	75.5	150	13.9
19c	CH_2OCONH_2		*c*Hex	119.7	0.34	352	0.34			
1				>200	0.12	>1666	0.7			
2				>200	0.03	>6666	0.2			
nevirapine				>200	0.25	>800				
S-1153[f]				22	0.003	7000	0.45	0.001[f]	0.009[f]	0.002[f]

[a] Data represent the mean value from three separate experiments; variation among triplicate samples was less than 15%. [b] CC_{50}: compound concentration required to reduce the viability of mock-infected cells by 50% (MTT method). [c] EC_{50}: compound concentration required to achieve 50% protection of MT-4 cells from HIV-1-induced cytopathicity (MTT method). [d] SI: selectivity index, ratio of CC_{50}/EC_{50}. [e] IC_{50}: compound concentration required to inhibit the HIV-1 rRT activity by 50%. [f] Published data refers to in vitro antiviral activity against resistant HIV strains (see references [15, 16]).

were found in the ester and alcohol series **17** and **18**, respectively.

Representative AThP derivatives were tested against the wild-type recombinant RT (rRT). All compounds inhibited the viral enzyme at concentrations similar to those active in cell-based assays. These results are expressed as IC_{50} values and are summarized in Table 1. Compounds **18b** and **19b** were the most potent derivatives in enzyme assays against wild-type RT. These derivatives were also tested against clinically relevant drug-resistant RT forms carrying the K103N, Y181I, and L100I mutations. Carbamate **19b** was 300–3500-fold less potent against the mutated rRTs than against wild-type rRT. Similar results were found for carbinol **18b** toward the K103N and Y181I mutants. In contrast, an interesting activity was detected for **18b** against L100I. In fact, this compound showed only a 14-fold loss in potency against this mutant with an EC_{50} value of 1.16 μM.

Molecular modeling

To gain insight as to the binding mode of these new AThP derivatives in the NNBS of HIV-1 RT, a docking study was undertaken for compounds **18b** and **19b** using the RT–S-1153 X-ray crystal structure (PDB code: 1EP4)[17] as a starting point. For compounds **10** and **14**, docking was also carried out in an attempt to elucidate the reasons behind the decreased biological activity. Docking experiments were carried out using the automated docking program GOLD 2.2.[25–29]

The top-ranked conformations of **18b** (GOLD fitness score = 51.88) and **19b** (GOLD fitness score = 49.87) docked similarly at the NNBS site, and their position in the active site was close to that of the co-crystallized inhibitor S-1153. Figure 4 shows the theoretical binding mode of **18b** and **19b** to the NNBS of HIV-1-RT. A schematic depiction of the interaction between both inhibitors and the RT NNBS residues is illustrated in Figure 5. It can be observed from Figure 4a that the hydroxy group of

 © 2006 Wiley-VCH Verlag GmbH & Co. KGaA, Weinheim

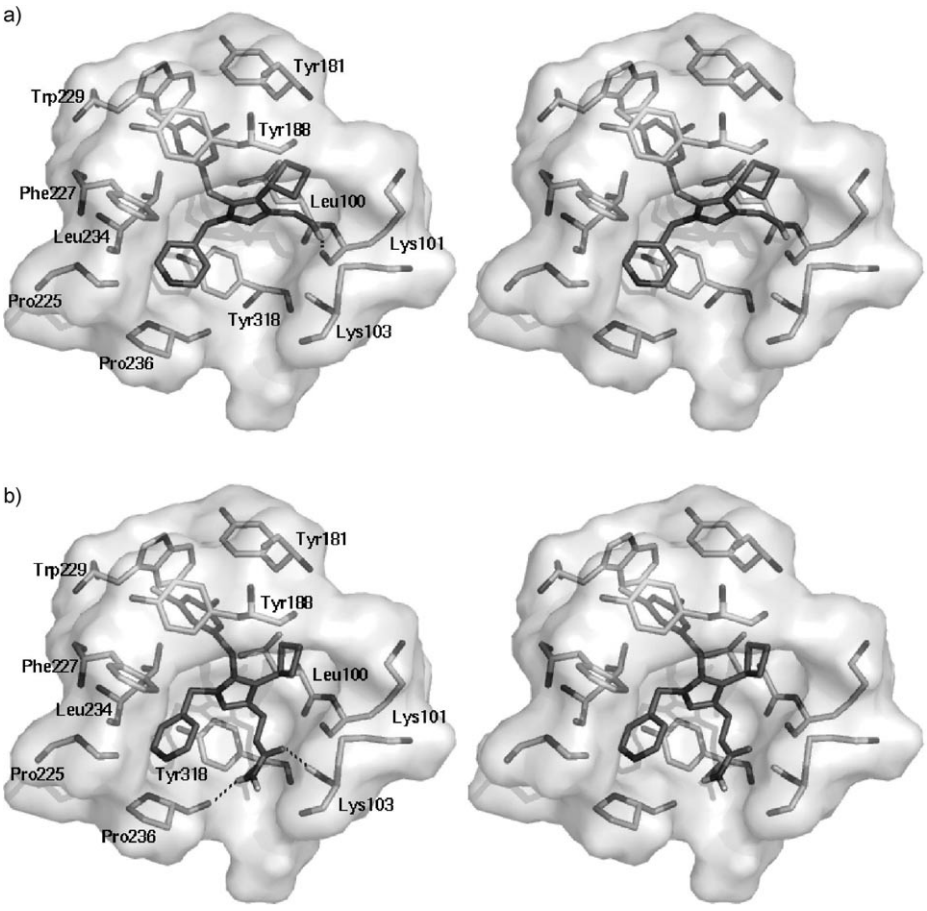

Figure 4. Stereographic views of the binding mode of compounds a) **18b** and b) **19b** into the NNBS cavity of HIV-1 RT. The protein residues within 3 Å from the docked ligands are shown and labeled. Ligands and interacting key residues are represented as stick models, and the protein, as a transparent Connolly surface. For clarity, only interacting polar hydrogen atoms are displayed. Hydrogen bonds are shown as dashed lines.

18b forms a hydrogen bond with the main chain C=O group of Lys 101 (OH···O=C $d = 2.0$ Å), whereas the carbamate group of **19b** is involved in two hydrogen bonds with the enzyme backbone: one involves the NH function and the main chain C=O group of Pro 236 (NH···O=C $d = 2.0$ Å), and the other occurs between the carbonyl oxygen atom and the main chain NH group of Lys 103 (C=O···HN $d = 1.9$ Å).

In each case, the cyclobutyl group of **18b** and **19b** is embedded within a hydrophobic pocket made up by the side chains of Leu 100, Gly 190, Val 106, and Val 179. The increased hydrophobic character of the cyclobutyl group in **18b** and **19b** relative to that of the isopropyl group of **1** and **2** and the deeper penetration into the hydrophobic pocket may explain the higher IC_{50} value of both **18b** and **19b** against RT than **1** and **2**. Replacement of the cyclobutyl group with the larger cyclohexyl ring (compounds **18c** and **19c**) would introduce small structural clashes in the NNRTI pocket, thus weakening antiviral activity.

The pyridinyl ring is hosted in a hydrophobic pocket made up by the side chains of Val 106, Pro 236, Pro 225, and Tyr 318, and also interacts with Phe 227 through a favorable T-shaped π–π contact. Finally, the 3,5-dichlorophenylthio moiety of both ligands is surrounded by the side chains of Tyr 181, Tyr 188, Phe 227, Trp 229, Leu 100, and Leu 234. Particularly, the electron-rich benzene rings of Tyr 188, Tyr 181, and Trp 299 appear to be optimally oriented for favorable π stacking and T-shaped π–π interactions with that (made electron-deficient by the two chlorine substituents) of both **18b** and **19b**.

Docking of compounds **10** and **14** into the RT NNBS did not converge toward a single binding position. In particular, the top-ranking solution of both compounds, having GOLD fitness scores of 45.21 and 44.44, respectively, resembled that of the co-crystallized inhibitor S-1153. In this binding pose, the carbonyl oxygen atom of the acetyl chain of **10** forms a hydrogen bond with the NH backbone portion of Lys 103, whereas the OCH_3 oxygen atom of the hydroxamate group of **14** forms a hydrogen bond with the Lys 101 backbone NH group. Inspection of the remaining docking solutions of the two compounds with lower GOLD fitness scores, revealed that they bind to the NNBS in a different pose without sharing the optimal interaction features reported for the compounds described so far. These results suggest that **10** and **14** could form a less stable complex with the RT NNBS, which explains why their activity is lower than that of compound **2**.

Regarding the effects of AThP derivatives against NNRTI-resistant HIV-1 strains, we reported in the accompanying paper that compound **5e** displays high activity against the K103N mutant.[19] Surprisingly, both inhibitors **18b** and **19b** are inactive against this mutation despite their structural similarity with compound **5e**. The low level of resistance observed for these two inhibitors might provide an indication that they interact slightly differently with the NNRTI binding pocket, and that the hydroxy and carbamate groups fail to disrupt the H bond between Asn 103 and Tyr 188 that stabilizes the unliganded (apoenzyme) form of the mutant enzyme.

Good activity against the L100I mutant was observed for **18b**, which showed only a 14-fold loss of potency against this mutant enzyme. Surprisingly, this mutation induced strong resistance against **19b**, resulting in a 347-fold lower IC_{50} for this inhibitor relative to its IC_{50} value toward wild-type RT. L100I is an isosteric replacement, though without adjustment. The branching at C^{β} rather than at C^{γ} would project the Ile γ-methyl group directly toward a portion of a given NNRTI and

 © 2006 Wiley-VCH Verlag GmbH & Co. KGaA, Weinheim

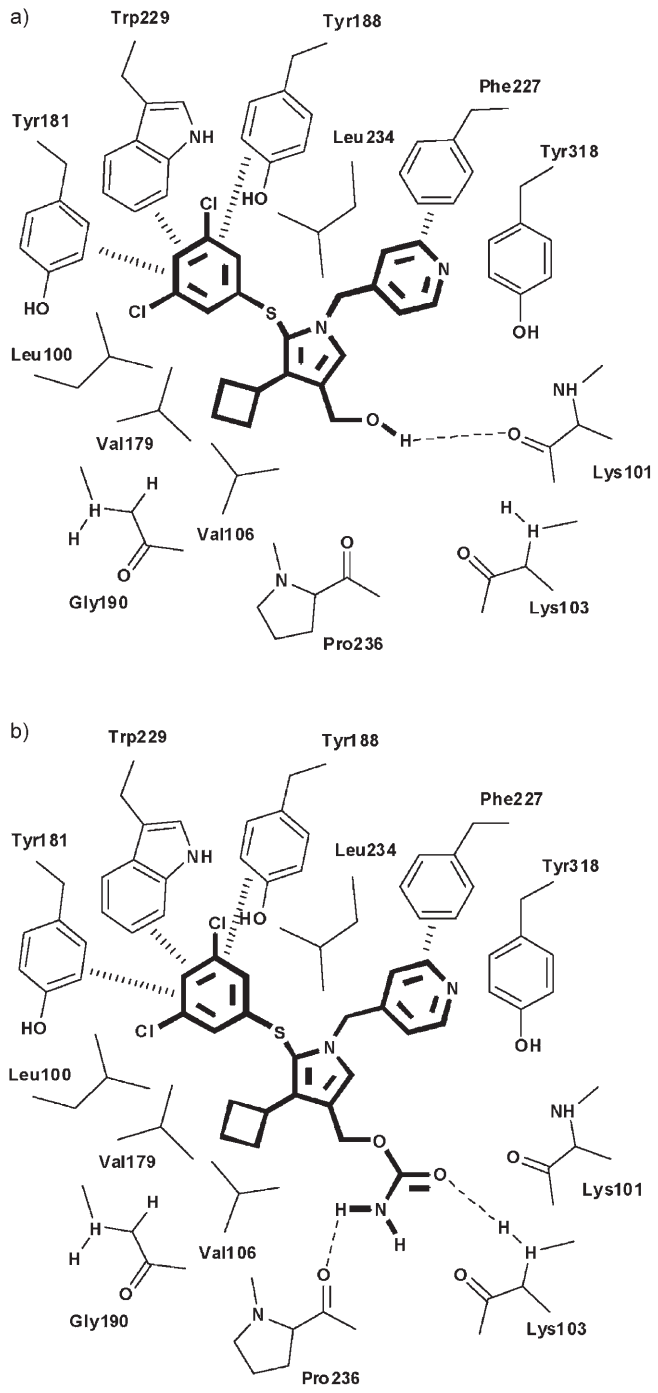

Figure 5. Possible interactions between the inhibitors a) **18b** and b) **19b**, and the surrounding residues of the HIV-1 RT NNBS.

adjacent to any group that H bonds with Lys 101. Thus, the L100I mutation is likely either to inflict unfavorable protein–ligand interactions or to destabilize the H bond with the backbone of Lys 101.[30,31] If an inhibitor reliant on this H bond is too large or inflexible, it will be vulnerable to this mutation.

Compound **18b** tolerates the L100I mutation fairly well because it is relatively flexible. A visual inspection of the **18b**–RT complex reveals that the ligand could be pressed a little deeper into the binding pocket, presumably to minimize the contact with the γ-methyl group, while retaining all key stabilizing interactions. In contrast, **19b** binds to the enzyme binding pocket in a slightly different orientation relative to **18b**. In fact, superimposition of both enzyme-bound conformations shows that there a lack of overlap precisely about the key functional groups. Nevertheless, each of these pharmacophoric functions engages the same enzyme side chain. Figure 6 shows the overlay of the receptor-bound ligands and selected residues of the enzyme binding site (Leu 100, Lys 101, Lys 103, and Pro 236).

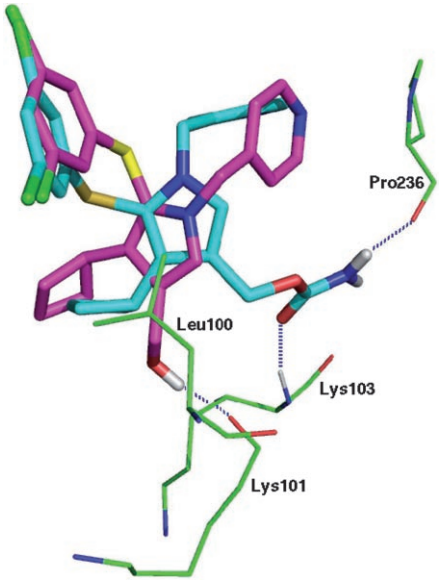

Figure 6. Overlay of the docked ligands **18b** (magenta) and **19b** (cyan). Only Leu 100, Lys 101, Lys 103, and Pro 236 residues are displayed (green).

Inspection of the **19b**–RT complex suggests that the γ-methyl group of Ile 100 probably gives rise to steric interference with the inhibitor, causing its repositioning or reorienting in the NNRTI pocket, which results in a significant loss in activity.

Conclusions

Docking models of the potent inhibitors **4k** and **5e** (accompanying paper)[19] with the NNBS of RT were employed to design novel AThP derivatives. The carbinol and carbamate group at position 3 of the pyrrole ring of **4k** and **5e** were replaced with a number of groups capable of forming H bonds. Unfortunately, none of these groups could effectively mimic the role of the carbamate group, and the most potent derivatives described herein (compounds **10** and **14**) were 3–15 times less potent than reference drugs **1** and **2**. On the other hand, the introduction of cycloalkyl groups at position 4 of the pyrrole ring of **1** and **2** led to derivatives **17**–**19**, which are endowed with potent antiviral activities. In particular, replacement of the isopropyl group with a cyclobutyl moiety gave **18b** and **19b**, which proved to be the most potent derivatives of this series. Compound **19b** was equipotent with the reference drug S-

 © 2006 Wiley-VCH Verlag GmbH & Co. KGaA, Weinheim

1153 (EC_{50} = 0.007 and 0.003 μM, respectively). The target of this AThP series was confirmed in enzyme assays against wild-type rRT, and the tested derivatives showed IC_{50} values that paralleled with EC_{50} values determined in cell-based assays, with a few exceptions. Moreover, the most potent derivatives in enzyme assays were tested against the clinically relevant drug-resistant RT forms carrying K103N, Y181I, and L100I mutations. Interestingly, **18b** and **19b** showed 14–3500-fold decreased potency against the above mutants relative to wild-type enzyme. Moreover, docking studies were performed with the aim to characterize the mode of binding of **10**, **14**, **18b**, and **19b** within the NNBS to rationalize both SAR data and potencies of the compounds against the mutants.

In conclusion, the AThP derivatives are interesting NNRTIs that are endowed with potent antiviral activities. Ongoing studies involve extension of the illustrated SAR strategy to identify additional activity parameters in the AThP series to overcome viral resistance.

Experimental Section

Materials: Melting points were determined on a Büchi 530 melting point apparatus and are uncorrected. IR spectra (nujol mulls) were recorded on a PerkinElmer 297 spectrophotometer. ^{1}H NMR spectra were recorded at 200 MHz on a Bruker AC 200 spectrometer using tetramethylsilane as internal reference standard. All compounds were routinely checked by TLC and ^{1}H NMR. TLC was performed with aluminum-baked silica gel plates (Fluka DC-Alufolien Kieselgel 60 F_{254}). Developed plates were visualized by UV light. Solvents were reagent grade and, when necessary, were purified and dried by standard methods. Concentration of solutions after reactions and extractions involved the use of a rotary evaporator (Büchi) operating at a reduced pressure (≈20 Torr). Organic solutions were dried over anhydrous sodium sulfate. Analytical results agreed to within ±0.40% of the theoretical values. All newly synthesized compounds **5**–**19** were analyzed for C, H, N, S, and, when present, Cl.

Syntheses: General procedure for the preparation of compounds **21a–c** and **24a,b**; example: ethyl 4-cyclopropyl-1*H*-pyrrole-3-carboxylate (**21a**). A solution of ethyl 3-cyclopropylacrylate **20a**[20] (5.0 g, 35.7 mmol) and TosMIC (7.7 g, 39.3 mmol) in an anhydrous mixture of DMSO/Et_2O (60:120 *v/v*) was added dropwise to a well-stirred suspension of sodium hydride (3.14 g, 78.5 mmol of 60% suspension in white oil) in anhydrous Et_2O (70 mL) under a stream of argon. After addition, the mixture was stirred at room temperature for 50 min, then treated with water (500 mL) and extracted with ethyl acetate (3×600 mL). The organic extracts were collected, washed with brine (6×300 mL), dried, and the solvent was evaporated under reduced pressure. The residue was separated on an aluminum oxide column (chloroform as eluent) to furnish pure **21a** (5.7 g, 89%); oil; IR: $\tilde{\nu}$ = 3315 (NH) and 1680 cm^{-1} (CO); ^{1}H NMR ($CDCl_3$): δ = 0.48 and 0.36 (2 m, 4H, CH_2), 1.38 (t, 3H, CH_3), 2.23 (m, 1H, CH), 4.29 (q, 2H, CH_2), 6.36 (m, 1H, pyrrole C5-H), 7.35 (m, 1H, pyrrole C2-H), 8.40 ppm (br s, 1H, NH).

Starting material; yield; reaction time; melting point; recrystallization solvent; IR spectroscopic data; and ^{1}H NMR spectroscopic data are listed for each of the following compounds:

21b: ethyl 3-cyclobutylacrylate (**20b**);[21] 34%; 40 min; 43–45 °C; *n*-hexane; IR: $\tilde{\nu}$ = 3220 (NH) and 1682 cm^{-1} (CO); ^{1}H NMR ($CDCl_3$): δ = 1.40 (t, 3H, CH_3), 1.85–2.45 (m, 6H, CH_2), 3.90 (m, 1H, CH), 4.31 (q, 2H, CH_2CH_3), 6.66 (m, 1H, pyrrole C5-H), 7.44 (m, 1H, pyrrole C2-H), 8.51 ppm (br s, 1H, NH).

21c: ethyl 3-cyclohexylacrylate (**20c**);[22] 67%; 25 min; 90–91 °C; cyclohexane; IR: $\tilde{\nu}$ = 3271 (NH) and 1660 cm^{-1} (CO); ^{1}H NMR ($CDCl_3$): δ = 1.22–2.08 (m, 13H, CH_3 and CH_2), 3.04 (m, 1H, CH), 4.31 (q, 2H, CH_2CH_3), 6.56 (m, 1H, pyrrole C5-H), 7.41 (m, 1H, pyrrole C2-H), 8.75 ppm (br s, 1H, NH).

24a: 5-methyl-3-hexen-2-one (**23a**);[23] 30%; 40 min; 99–102 °C; cyclohexane; IR: $\tilde{\nu}$ = 3144 (NH) and 1625 cm^{-1} (CO); ^{1}H NMR ($CDCl_3$): δ = 1.26 (d, 6H, CH_3), 2.47 (s, 3H, $COCH_3$), 3.53 (m, 1H, CH), 6.66 (m, 1H, pyrrole C5-H), 7.43 (m, 1H, pyrrole C2-H), 8.79 ppm (br s, 1H, NH).

24b: 4-methyl-1-phenyl-2-penten-1-one (**23b**);[24] 39%; 1 h; 144–146 °C; benzene; IR: $\tilde{\nu}$ = 3140 (NH) and 1580 cm^{-1} (CO); ^{1}H NMR ($CDCl_3$): δ = 1.29 (d, 6H, CH_3), 3.64 (m, 1H, CH), 6.68 (m, 1H, pyrrole C5-H), 7.07–7.99 (m, 6H, benzene C-H and pyrrole C2-H), 8.78 ppm (br s, 1H, NH).

General procedure for the preparation of compounds **22a–c** and **25a,b**; example: ethyl 4-cyclopropyl-5-(3,5-dicholorophenylthio)-1*H*-pyrrole-3-carboxylate (**22a**). A solution of potassium iodide (9.3 g, 0.056 mol) and iodine (2.9 g, 0.011 mol) in aqueous ethanol (50%, 35 mL) was added dropwise to a well-stirred solution of **21a** (2.0 g, 0.011 mol) and 3,5-dichorothiophenol (2.0 g, 0.011 mol) in the same solvent (50 mL) under argon atmosphere. The mixture was kept at reflux for 2.5 h, cooled, and treated with water (100 mL). The suspension that formed was extracted with ethyl acetate (3×100 mL), and the organic extracts were collected, washed with a solution of 0.2 N sodium thiosulfate (3×200 mL), then with brine (3×200 mL), and dried. The crude product was separated on a silica gel column (chloroform as eluent) to obtain pure **22a** (3.9 g, 100%); mp: 117–119 °C (from cyclohexane); IR: $\tilde{\nu}$ = 3250 (NH) and 1670 cm^{-1} (CO); ^{1}H NMR ($CDCl_3$): δ = 0.91–0.96 (m, 4H, CH_2), 1.42 (t, 3H, CH_3), 2.25 (m, 1H, CH), 4.35 (q, 2H, CH_2), 6.84–6.85 (m, 2H, benzene C2-H and C6-H), 7.15 (m, 1H, benzene C4-H), 7.60 (m, 1H, pyrrole C2-H), 8.50 ppm (br s, 1H, NH).

Yield; reaction time; chromatographic system; melting point; recrystallization solvent; IR spectroscopic data; and ^{1}H NMR spectroscopic data are listed for each of the following compounds:

22b: 76%; 3.5 h; SiO_2 (chloroform); 114–116 °C; cyclohexane; IR: $\tilde{\nu}$ = 3210 (NH) and 1684 cm^{-1} (CO); ^{1}H NMR ($CDCl_3$): δ = 1.43 (t, 3H, CH_3), 1.88–2.66 (m, 6H, CH_2), 4.07 (m, 1H, CH), 4.36 (q, 2H, CH_2CH_3), 6.86 (m, 2H, benzene C2-H and C6-H), 7.15 (m, 1H, benzene C4-H), 7.62 (d, 1H, $J_{1,2}$ = 3.3 Hz, pyrrole C2-H), 8.54 ppm (br s, 1H, NH).

22c: 57%; 3.5 h; SiO_2 (chloroform); 177–178 °C; benzene/cyclohexane; IR: $\tilde{\nu}$ = 3229 (NH) and 1681 cm^{-1} (CO); ^{1}H NMR ($CDCl_3$): δ = 1.30–2.03 (m, 13H, CH_3 and CH_2), 3.28 (m, 1H, CH), 4.35 (q, 2H, CH_2CH_3), 6.83 (m, 2H, benzene C2-H and C6-H), 7.12 (m, 1H, benzene C4-H), 7.62 (d, 1H, $J_{1,2}$ = 3.3 Hz, pyrrole C2-H), 8.40 ppm (br s, 1H, NH).

25a: 40%; 6.5 h; SiO_2 (chloroform); 150–152 °C; cyclohexane; IR: $\tilde{\nu}$ = 3250 (NH) and 1620 cm^{-1} (CO); ^{1}H NMR ($CDCl_3$): δ = 1.34 (d, 6H, CH_3), 2.52 (s, 3H, $COCH_3$), 3.66 (m, 1H, CH), 6.85 (m, 2H, benzene C2-H and C6-H), 7.16 (m, 1H, benzene C4-H), 7.61 (d, 1H, $J_{1,2}$ = 3.3 Hz, pyrrole C2-H), 8.34 ppm (br s, 1H, NH).

25b: 22%; 3 h; SiO_2 (chloroform/light petroleum ether, 1:1); 165–167 °C; benzene; IR: $\tilde{\nu}$ = 3120 (NH) and 1590 cm^{-1} (CO); ^{1}H NMR

 © 2006 Wiley-VCH Verlag GmbH & Co. KGaA, Weinheim

($CDCl_3$): $\delta = 1.39$ (d, 6H, CH_3), 3.66 (m, 1H, CH), 6.88–7.70 (m, 9H, benzene C-H and pyrrole C2-H), 8.55 ppm (br s, 1H, NH).

General procedure for the preparation of compounds **6**, **7**, and **17a–c**; example: ethyl 4-cyclopropyl-5-(3,5-dicholorophenylthio)-1-(4-pyridinylmethyl)-1*H*-pyrrole-3-carboxylate (**17a**). A well-cooled solution of tetrabutylammonium hydrogen sulfate (1.7 g, 5.2 mmol) and 4-(chloromethyl)pyridine hydrochloride (0.8 g, 5.2 mmol) in dichloromethane (10 mL) was treated with sodium hydroxide (50%, 10 mL) and with a solution of **22a** (1.8 g, 5.2 mmol) in dichloromethane (15 mL), in turn. The mixture was stirred at room temperature for 1 h, then water (50 mL) was added and the suspension that formed was extracted with chloroform (3×50 mL). The organic extracts were collected, washed with brine, and dried. The evaporation of the solvent gave the crude product, which was separated on a silica gel column (ethyl acetate as eluent) to give pure **17a** (1.5 g, 64%); mp: 114–116 °C (from *n*-hexane); IR: $\tilde{\nu} =$ 1712 cm^{-1} (CO); ^1H NMR ($CDCl_3$): $\delta = 0.91$–0.99 (m, 4H, CH_2), 1.41 (t, 3H, CH_3), 2.30 (m, 1H, CH), 4.35 (q, 2H, CH_2CH_3), 5.11 (s, 2H, CH_2), 6.68 (m, 2H, benzene C2-H and C6-H), 6.88 (m, 2H, pyridine C3-H and C5-H), 7.07 (m, 1H, benzene C4-H), 7.65 (s, 1H, pyrrole C2-H), 8.50 ppm (m, 2H, pyridine C2-H and C6-H).

Yield; reaction time; chromatographic system; melting point; recrystallization solvent; IR spectroscopic data; and ^1H NMR spectroscopic data are listed for each of the following compounds:

6: 75%; 2.5 h; SiO_2 (ethyl acetate); 150–152 °C; cyclohexane; IR: $\tilde{\nu} = 1650$ cm^{-1} (CO); ^1H NMR ($CDCl_3$): $\delta = 1.36$ (d, 6H, CH_3), 2.52 (s, 3H, $COCH_3$), 3.65 (m, 1H, CH), 5.20 (s, 2H, CH_2), 6.70 (m, 2H, benzene C2-H and C6-H), 6.98 (m, 2H, pyridine C3-H and C5-H), 7.09 (m, 1H, benzene C4-H), 7.66 (s, 1H, pyrrole C2-H), 8.56 ppm (m, 2H, pyridine C2-H and C6-H).

7: 88%; 1.5 h; SiO_2 (ethyl acetate); oil; IR: $\tilde{\nu} = 1620$ cm^{-1} (CO); ^1H NMR ($CDCl_3$): $\delta = 1.41$ (d, 6H, CH_3), 3.60 (m, 1H, CH), 5.14 (s, 2H, CH_2), 6.72 (m, 2H, phenylthio C2-H and C6-H), 6.87 (m, 2H, pyridine C3-H and C5-H), 7.07 (m, 1H, phenylthio C4-H), 7.30–7.85 (m, 5H, benzene C-H), 8.04 (s, 1H, pyrrole C2-H), 8.49 ppm (m, 2H, pyridine C2-H and C6-H).

17b: 63%; 1.5 h; SiO_2 (chloroform/ethyl acetate, 1:9); 123–125 °C; cyclohexane; IR: $\tilde{\nu} = 1710$ cm^{-1} (CO); ^1H NMR ($CDCl_3$): $\delta = 1.42$ (t, 3H, CH_3), 1.75–2.66 (m, 6H, CH_2), 4.10 (m, 1H, CH), 4.37 (q, 2H, CH_2CH_3), 5.13 (s, 2H, CH_2), 6.68 (m, 2H, benzene C2-H and C6-H), 6.89 (m, 2H, pyridine C3-H and C5-H), 7.07 (m, 1H, benzene C4-H), 7.67 (s, 1H, pyrrole C2-H), 8.49 ppm (m, 2H, pyridine C2-H and C6-H).

17c: 75%; 1.5 h; SiO_2 (ethyl acetate); 116–117 °C; *n*-hexane; IR: $\tilde{\nu} =$ 1712 cm^{-1} (CO); ^1H NMR ($CDCl_3$): $\delta = 1.32$–2.09 (m, 13H, CH_3 and CH_2), 3.29 (m, 1H, CH), 4.34 (q, 2H, CH_2CH_3), 5.10 (s, 2H, CH_2), 6.65 (m, 2H, benzene C2-H and C6-H), 6.88 (m, 2H, pyridine C3-H and C5-H), 7.04 (m, 1H, benzene C4-H), 7.67 (s, 1H, pyrrole C2-H), 8.49 ppm (m, 2H, pyridine C2-H and C6-H).

General procedure for the preparation of compounds **18a–c**; example: 4-cyclopropyl-5-(3,5-dicholorophenylthio)-1-(4-pyridinylmethyl)-1*H*-pyrrole-3-methanol (**18a**). A solution of **17a** (0.9 g, 2.0 mmol) in anhydrous tetrahydrofuran (70 mL) was added dropwise to a well-stirred suspension of lithium aluminum hydride (0.4 g, 10.5 mmol) in the same solvent (70 mL) cooled at 0 °C. After addition, the mixture was stirred at room temperature for 18 h and then carefully treated with crushed ice. The inorganic precipitate was removed, and the solution was concentrated and treated with ethyl acetate (100 mL). The organic solution was shaken with brine (3×100 mL), dried, and evaporated to give crude product, which was separated on a silica gel column (ethyl acetate as eluent) to obtain pure **18a** (0.2 g, 24%); mp: 115–116 °C (from cyclohexane); IR: $\tilde{\nu} = 3300$ cm^{-1} (OH); ^1H NMR ($CDCl_3$): $\delta = 0.86$ (m, 4H, CH_2), 2.00 (br s, 1H, OH), 2.20 (m, 1H, CH), 4.70 (s, 2H, CH_2OH), 5.08 (s, 2H, NCH_2), 6.82–7.30 (m, 6H, pyridine C3-H and C5-H, pyrrole C2-H and benzene C-H), 8.45 ppm (m, 2H, pyridine C2-H and C6-H).

Yield; reaction time; chromatographic system; melting point; recrystallization solvent; IR spectroscopic data; and ^1H NMR spectroscopic data are listed for each of the following compounds:

18b: 51%; 3.5 h; SiO_2 (ethyl acetate); oil; IR: $\tilde{\nu} = 3280$ cm^{-1} (OH); ^1H NMR ($CDCl_3$): $\delta = 1.85$–2.48 (m, 6H, CH_2), 3.00 (br s, 1H, OH), 3.74 (m, 1H, CH), 4.80 (s, 2H, CH_2OH), 5.18 (s, 2H, NCH_2), 6.71 (m, 2H, benzene C2-H and C6-H), 7.07–7.12 (m, 4H, pyridine C3-H and C5-H, pyrrole C2-H and benzene C4-H), 8.55 ppm (m, 2H, pyridine C2-H and C6-H).

18c: 35%; 2 h; SiO_2 (ethyl acetate); 55–57 °C; cyclohexane; IR: $\tilde{\nu} =$ 3250 cm^{-1} (OH); ^1H NMR ($CDCl_3$): $\delta = 1.25$–1.80 (m, 10H, CH_2), 2.05 (br s, 1H, OH), 2.85 (m, 1H, CH), 4.74 (s, 2H, CH_2OH), 5.07 (s, 2H, NCH_2), 6.67 (m, 2H, benzene C2-H and C6-H), 6.88 (m, 2H, pyridine C3-H and C5-H), 7.02–7.04 (m, 2H, pyrrole C2-H and benzene C4-H), 8.44 ppm (m, 2H, pyridine C2-H and C6-H).

General procedure for the preparation of compounds **19a–c**; example: 4-cyclopropyl-5-(3,5-dicholorophenylthio)-1-(4-pyridinylmethyl)-1*H*-pyrrole-3-methanol carbamate (**19a**). Trichloroacetyl isocyanate (100 mg, 0.5 mmol) was added dropwise to a well-stirred solution of **18a** (200 mg, 0.5 mmol) in dichloromethane (3 mL) cooled at 0 °C. The mixture was then stirred at room temperature for 1.5 h, and the solvent was removed under reduced pressure. The residue was dissolved in methanol (1 mL), and the resulting solution was cooled at 0 °C and treated with a cold solution of potassium carbonate (250 mg, 1.8 mmol) in water (1 mL). The resulting suspension was stirred at room temperature for 3.5 h, then the methanol was removed under reduced pressure, and the residue was treated with ethyl acetate (100 mL). The organic solution was washed with brine (3×20 mL) and dried. Evaporation of the solvent gave the crude product, which was separated on a silica gel column (ethyl acetate as eluent) to give pure **19a** (130 mg, 58%); mp: 118–120 °C (from cyclohexane); IR: $\tilde{\nu} = 3300$, 3130 (NH_2) and 1695 cm^{-1} (CO); ^1H NMR ($CDCl_3$): $\delta = 0.76$–0.89 (m, 4H, CH_2), 1.78 (m, 1H, CH), 4.73 (br s, 2H, NH_2), 5.08 (s, 2H, CH_2OCONH_2), 5.13 (s, 2H, NCH_2), 6.68 (m, 2H, benzene C2-H and C6-H), 6.88 (m, 2H, pyridine C3-H and C5-H), 7.04–7.08 (m, 2H, pyrrole C2-H and benzene C4-H), 8.48 ppm (m, 2H, pyridine C2-H and C6-H).

Yield; chromatographic system; melting point; recrystallization solvent; IR spectroscopic data; and ^1H NMR spectroscopic data are listed for each of the following compounds:

19b: 29%; SiO_2 (ethyl acetate); 146–147 °C; cyclohexane; IR: $\tilde{\nu} =$ 3300, 3140 (NH_2) and 1696 cm^{-1} (CO); ^1H NMR ($CDCl_3$): $\delta = 1.76$–2.31 (m, 6H, CH_2), 3.59 (m, 1H, CH), 4.60 (br s, 2H, NH_2), 4.99 (s, 2H, CH_2OCONH_2), 5.06 (s, 2H, NCH_2), 6.55 (m, 2H, benzene C2-H and C6-H), 6.80 (m, 2H, pyridine C3-H and C5-H), 6.94 (m, 1H, benzene C4-H), 6.98 (s, 1H, pyrrole C2-H), 8.37 ppm (m, 2H, pyridine C2-H and C6-H).

19c: 66%; SiO_2 (ethyl acetate); 100–102 °C; cyclohexane; IR: $\tilde{\nu} =$ 3320, 3120 (NH_2) and 1713 cm^{-1} (CO); ^1H NMR ($CDCl_3$): $\delta = 1.30$–1.76 (m, 10H, CH_2), 2.80 (m, 1H, CH), 4.97–5.18 (m, 6H, CH_2OCONH_2, NCH_2 and NH_2), 6.64–7.14 (m, 6H, benzene C-H, pyridine C3-H and C5-H and pyrrole C2-H), 8.47 ppm (m, 2H, pyridine C2-H and C6-H).

 © 2006 Wiley-VCH Verlag GmbH & Co. KGaA, Weinheim

General procedure for the preparation of compounds **8** and **9**; example: 5-(3,5-dicholorophenylthio)-4-isopropyl-1-(4-pyridinylmethyl)-1*H*-pyrrole-3-ethanol (**8**). A solution of **6** (1.0 g, 2.4 mmol) in methanol (13 mL) was cooled at 0 °C and treated with sodium borohydride (450 mg, 11.9 mmol). The mixture was stirred at the same temperature for 1.5 h, then water was added (100 mL), and the precipitate that formed was extracted with ethyl acetate (3× 50 mL). The organic solutions were collected, washed with brine (3×100 mL), dried, and evaporated to give crude product, which was separated on a silica gel column (ethyl acetate/*n*-hexane 5:1 as eluent) to obtain pure **8** (0.8 g, 80%); mp: 148–150 °C (from cyclohexane); IR: $\tilde{\nu}=3190\ cm^{-1}$ (OH); ^1H NMR ($CDCl_3$): $\delta=1.32$ (m, 6H, $CHCH_3$), 1.59 (d, 3H, $CHOHCH_3$), 2.30 (br s, 1H, OH), 3.20 (m, 1H, $CHCH_3$), 5.07–5.20 (m, 3H, $CHOHCH_3$ and CH_2), 6.65 (m, 2H, benzene C2-H and C6-H), 6.87 (m, 2H, pyridine C3-H and C5-H), 7.03 (m, 1H, benzene C4-H), 7.07 (s, 1H, pyrrole C2-H), 8.43 ppm (m, 2H, pyridine C2-H and C6-H).

Yield; reaction time; chromatographic system; melting point; recrystallization solvent; IR spectroscopic data; and ^1H NMR spectroscopic data are listed for the following compound:

9: 18%; 72 h; SiO_2 (ethyl acetate/chloroform 1:1); 129–130 °C; cyclohexane; IR: $\tilde{\nu}=3180\ cm^{-1}$ (OH); ^1H NMR ($CDCl_3$): $\delta=1.25$ (m, 6H, CH_3), 1.80 (br s, 1H, OH), 3.20 (m, 1H, $CHCH_3$), 5.04 (s, 2H, CH_2), 6.07 (s, 1H, $CHOH$), 6.65 (m, 2H, phenylthio C2-H and C6-H), 6.83 (m, 2H, pyridine C3-H and C5-H), 7.05 (m, 1H, phenylthio C4-H), 7.30–7.53 (m, 6H, benzene C-H, and pyrrole C2-H), 8.45 ppm (m, 2H, pyridine C2-H and C6-H).

General procedure for the preparation of compounds **11** and **12**; 4-isopropyl-5-phenylthio-1-(4-pyridinylmethyl)-1*H*-pyrrole-3-carboxylic acid (**11**). A well-stirred solution of **26**[18] (3.0 g, 7.9 mmol) in ethanol (30 mL) was treated with sodium hydroxide (20%, 20.5 mL). The mixture was kept at reflux for 2.5 h, then was cooled and treated with 1 N HCl to bring the solution to pH 4. The precipitate that formed was filtered and washed with light petroleum ether, then dried with an IR lamp to obtain pure acid **11** (2.0 g, 72%); mp: 170–172 °C (from benzene/cyclohexane); IR: $\tilde{\nu}=3000$ (OH) and 1710 cm^{-1} (CO); ^1H NMR ($CDCl_3$): $\delta=1.32$ (d, 6H, CH_3), 3.67 (m, 1H, CH), 5.09 (s, 2H, CH_2), 6.84–6.91 (m, 4H, pyridine C3-H and C5-H and benzene C2-H and C6-H), 7.03–7.20 (m, 3H, benzene C3-H, C4-H and C5-H), 7.66 (s, 1H, pyrrole C2-H), 8.46–8.49 ppm (m, 2H, pyridine C2-H and C6-H).

Yield; chromatographic system; melting point; recrystallization solvent; IR spectroscopic data; and ^1H NMR spectroscopic data are listed for the following compound:

12: 77%; SiO_2 (ethyl acetate); 108–110 °C; benzene/cyclohexane; IR: $\tilde{\nu}=3000$ (OH) and 1710 cm^{-1} (CO); ^1H NMR ($CDCl_3$): $\delta=1.38$ (d, 6H, CH_3), 3.64 (m, 1H, CH), 5.15 (s, 2H, CH_2), 6.68 (m, 2H, benzene C2-H and C6-H), 6.95 (m, 2H, pyridine C3-H and C5-H), 7.06 (m, 1H, benzene C4-H), 7.79 (s, 1H, pyrrole C2-H), 8.54 ppm (m, 2H, pyridine C2-H and C6-H).

General procedure for the preparation of compounds **13**–**16**; example: 4-isopropyl-*N*-methyl-5-phenylthio-1-(4-pyridinylmethyl)-1*H*-pyrrole-3-carboxylic acid hydrazide (**15**). EDCI (480 mg, 25 mmol) was added to a well-stirred solution of **11** (700 mg, 2.0 mmol), HOBT (270 mg, 2.0 mmol), NMM (960 mg, 9.5 mmol), and methyl hydrazine (260 mg, 5.7 mmol) in dichloromethane (35 mL). The mixture was stirred at room temperature for 15 h, then water was added (50 mL), and the precipitate that formed was extracted with chloroform (3×50 mL). The collected organic extracts were washed with brine (3×100 mL), dried, and the solvent was removed under reduced pressure to furnish the crude product, which was separated on a silica gel column (dichloromethane/methanol 20:0.5 as eluent) to obtain pure **15** (250 mg, 33%); mp: 81–83 °C (from benzene/cyclohexane); IR: $\tilde{\nu}=3220$, 3120 (NH) and 1600 cm^{-1} (CO); ^1H NMR ($CDCl_3$): $\delta=1.28$ (d, 6H, CH_3), 3.13–3.29 (m, 4H, $NHCH_3$ and CH), 4.57 (br s, 2H, NH), 5.00 (s, 2H, CH_2), 6.78–7.52 (m, 8H, benzene C-H, pyrrole C2-H, and pyridine C3-H and C5-H), 8.43 ppm (m, 2H, pyridine C2-H and C6-H).

Reagent; yield; chromatographic system; melting point; recrystallization solvent; IR spectroscopic data; and ^1H NMR spectroscopic data are listed for each of the following compounds:

13: methyl hydroxylamine; 18%; 172–174 °C; benzene; IR: $\tilde{\nu}=3080$ (NH) and 1630 cm^{-1} (CO); ^1H NMR ($CDCl_3$): $\delta=1.35$ (d, 6H, CH_3), 3.48 (m, 1H, CH), 3.85 (s, 3H, OCH_3), 5.06 (s, 2H, CH_2), 6.81–7.21 (m, 8H, benzene C-H, pyrrole C2-H, and pyridine C3-H and C5-H), 8.39 (m, 2H, pyridine C2-H and C6-H), 8.71 ppm (br s, 1H, NH).

14: methyl hydroxylamine; 45%; 128–129 °C; benzene; IR: $\tilde{\nu}=3120$ (NH) and 1620 cm^{-1} (CO); ^1H NMR ($CDCl_3$): $\delta=1.34$ (d, 6H, CH_3), 3.45 (m, 1H, CH), 3.86 (s, 3H, OCH_3), 5.07 (s, 2H, CH_2), 6.65 (m, 2H, benzene C2-H and C6-H), 6.83 (m, 2H, pyridine C3-H and C5-H), 7.03 (m, 1H, benzene C4-H), 7.36 (s, 1H, pyrrole C2-H), 8.38 ppm (m, 2H, pyridine C2-H and C6-H).

16: methyl hydrazine; 69%; 140–142 °C; benzene/cyclohexane; IR: $\tilde{\nu}=3210$, 3100 (NH) and 1605 cm^{-1} (CO); ^1H NMR ($CDCl_3$): $\delta=1.22$ (d, 6H, CH_3), 3.03–3.28 (m, 4H, $NHCH_3$ and CH), 4.51 (br s, 2H, NH), 5.01 (s, 2H, CH_2), 6.57 (m, 2H, benzene C2-H and C6-H), 6.79 (m, 2H, pyridine C3-H and C5-H), 6.94 (m, 1H, benzene C4-H), 7.01 (s, 1H, pyrrole C2-H), 8.38 ppm (m, 2H, pyridine C2-H and C6-H).

4-Ethoxymethyl-3-isopropyl-2-phenylthio-1-(4-pyridinylmethyl)-1*H*-pyrrole (**5**): a well-stirred solution of **4**[18] (380 mg, 1.1 mmol) in anhydrous ethanol (2 mL), cooled at 0 °C, was carefully treated with HCl (conc., 0.1 mL). The mixture was stirred at room temperature for 20 min, then Et_2O was added (20 mL), and the precipitate that formed was filtered to obtain crude product, which was separated on a silica gel column (ethyl acetate as eluent) to obtain pure **5** (340 mg, 83%); oil; ^1H NMR ($CDCl_3$): $\delta=1.22$–1.30 (m, 9H, CH_3), 3.24 (m, 1H, CH), 3.58 (q, 2H, CH_2CH_3), 4.47 (s, 2H, OCH_2), 5.03 (s, 2H, NCH_2), 6.77–7.21 (m, 8H, benzene C-H, pyridine C3-H and C5-H and pyrrole C2-H), 8.42 ppm (m, 2H, pyridine C2-H and C6-H).

4-Acetoxymethyl-3-isopropyl-2-phenylthio-1-(4-pyridinylmethyl)-1*H*-pyrrole (**10**): TEA (210 mg, 2.1 mmol) and DMAP (8 mg, 0.07 mmol) were added to a solution of **4**[18] (500 mg, 1.5 mmol) in acetic anhydride (0.2 mL). The mixture was stirred at room temperature for 20 min, then carefully treated with crushed ice. The solution was concentrated and treated with ethyl acetate (100 mL). The collected organic extracts were washed with brine (3×100 mL), dried, and the solvent was removed under reduced pressure to furnish the crude product, which was separated on a silica gel column (acetate as eluent) to obtain pure **10** (550 mg, 98%); oil; ^1H NMR ($CDCl_3$): $\delta=1.31$–1.40 (m, 6H, CH_3), 2.17 (s, 3H, $COCH_3$), 3.24 (m, 1H, CH), 3.38 (m, 1H, CH), 5.18 and 5.36 (2 s, 4H, CH_2), 6.85–7.42 (m, 8H, benzene C-H, pyridine C3-H and C5-H and pyrrole C2-H), 8.52 ppm (m, 2H, pyridine C2-H and C6-H).

Microbiology: For the antiviral assays, all compounds were solubilized in DMSO at 200 μM and then diluted in culture medium.

Cells and viruses: MT-4 cells were grown at 37 °C in a CO_2 atmosphere (5%) in RPMI 1640 medium supplemented with fetal calf serum (FCS, 10%), penicillin G (100 IU ml^{-1}), and streptomycin (100 μg mL^{-1}). Cell cultures were checked periodically for the ab-

 © 2006 Wiley-VCH Verlag GmbH & Co. KGaA, Weinheim

sence of mycoplasma contamination with a MycoTect Kit (Gibco). Human immunodeficiency viruses type-1 (HIV-1, IIIB strain) was obtained from supernatants of persistently infected cells. HIV-1 stock solutions had titers of 1.5×10^7 mL^{-1} for a 50% cell culture infectious dose ($CCID_{50}$).

HIV titration: Titration of HIV was performed in C8166 cells by the standard limiting dilution method (dilution 1:2, four replica wells per dilution) in 96-well plates. The infectious virus titer was determined by light microscope scoring of syncytia after four days of incubation. Virus titers were expressed as $CCID_{50}$ per mL.

Anti-HIV assays: The activity of the compounds against multiplication of wild-type HIV-1 in acutely infected cells was based on the inhibition of virus-induced cytopathicity in MT-4 cells. Briefly, culture medium (50 μL) containing 1×10^4 cells was added to the wells of flat-bottom microtiter trays containing 50 μL culture medium with or without various concentrations of test compounds. Then, HIV suspensions (20 μL, each containing the appropriate amount (by $CCID_{50}$) to cause complete cytopathicity at day 4) were added. After incubation at 37 °C, cell viability was determined by the 3-(4,5-dimethylthiazol-1-yl)-2,5-diphenyltetrazolium bromide (MTT) method.[32] The cytotoxicity of each test compound was evaluated in parallel with its antiviral activity and was based on the viability of mock-infected cells, as monitored by the MTT method.

RT assays: Assays were performed as previously described.[33] Briefly, purified rRT (20–50 nM) was assayed for its RNA-dependent DNA polymerase activity in a volume of 25 μL containing Tris-HCl (50 mM, pH 7.8), KCl (80 mM), $MgCl_2$ (6 mM), DTT (1 mM), BSA (0.1 mg mL^{-1}), template–primer duplex: [poly(rA)–oligo(dT)$_{12-18}$] (0.3 μM, determined by 3′-OH end concentration), and [^{3}H]dTTP (10 μM, 1 Ci mmole^{-1}). After a incubation at 37 °C for 30 min, samples were spotted onto glass fiber filters (Whatman GF/C) and the acid-insoluble radioactivity was determined.

Computational chemistry: Molecular modeling and graphics manipulations were performed using the SYBYL software package (Sybyl Molecular Modeling System, version 6.9, Tripos Inc., St. Louis, USA), on a Silicon Graphics Tezro workstation equipped with four 700 MHz R16000 processors. Model building of **10**, **14**, **18b**, and **19b** was accomplished with the TRIPOS force field[34] available within SYBYL. Energy minimizations were realized by employing the INSIGHT II/DISCOVER program (Insight II Molecular Modeling Package and Discover 2.2000 Simulation Package, MSI Inc., San Diego, USA), selecting the CVFF force field.[35] Figures 3, 4, and 6 were made using PYMOL software.[36]

Docking simulations: Automated docking studies were performed with the docking algorithm GOLD 2.2.[25–29] This automated ligand-docking program uses a genetic algorithm to explore the full range of ligand conformational flexibility with partial flexibility of the receptor. GOLD requires a user-defined binding site. It searches for a cavity within the defined area and considers all the solvent-accessible atoms in the defined area as active-site atoms. On the basis of the GOLD score, for each molecule a bound conformation with high score was considered as the best bound conformation. The score function that was implemented in GOLD consisted basically of H bonding, complex energy, and ligand internal energy terms. A population of possible docked orientations of the ligand is set up at random. Each member of the population is encoded as a "chromosome", which contains information about the mapping of ligand H bond atoms onto (complementary) protein H bond atoms, mapping of hydrophobic points on the ligand onto protein hydrophobic points, and the conformation around flexible ligand bonds and protein OH groups. A number of parameters control the precise operation of the genetic algorithm.

Ligand setup: The core structures of ligands **10**, **14**, **18b**, and **19b** were built using standard bond lengths and bond angles of the SYBYL fragment library. Geometry optimizations were carried out with the SYBYL/MAXIMIN2 minimizer by applying the BFGS (Broyden, Fletcher, Goldfarb, and Shannon) algorithm and setting a rms gradient of the forces acting on each atom of 0.05 kcal mol^{-1} Å^{-1} as the convergence criterion.

Protein setup: The crystal structure of RT–S-1153 (PDB code: 1EP4)[17] recovered the Brookhaven Protein Data Bank was used. The structure was set up for docking as follows: polar and nonpolar hydrogen atoms were added using the BIOPOLYMERS module within SYBYL program (residues Arg, Lys, Glu, and Asp were considered ionized, whereas all His were considered neutral by default) and all water molecules were removed.

GOLD docking: An active site of radius 15 Å was defined considering the backbone C=O oxygen atom of Phe 227 as the center of the NNBS. 50 independent docking runs were performed for each docking experiment. All docking runs were carried out using standard default settings with a population size of 100, a maximum number of 100 000 operations, and a mutation and crossover rate of 95. The best generated 10 solutions of each ligand were ranked according to their fitness scores calculated by the GOLD ChemScore function.

To determine whether or not to include the two water molecules found in the RT–S-1153 crystal structure in docking experiments, an active site containing the two water molecules was first defined. The seven highest-scoring solutions found by GOLD were almost identical, and each reproduced the crystallographically determined position and conformation of S-1153 in the NNBS binding site with <0.6 Å rms deviation. To determine the minimum number and combination of water molecules required, water molecules were then systematically removed, giving active sites with combinations of one and zero water molecules in place, and S-1153 was redocked each time. These experiments showed that the position of S-1153 in the active site could be reliably reproduced by docking to a protein with no water molecules in the site.

Energy refinement of the 18b–RT and 19b–RT complexes: To eliminate any residual geometric strain, the obtained complexes were energy minimized using 3000 steps of steepest descent followed by 2000 of conjugate gradient, permitting only the ligand and the protein side chain atoms to relax. The geometry optimization was carried out employing the DISCOVER program with the CVFF force field.

Acknowledgements

Thanks are due to the Italian Ministero della Sanità—Istituto Superiore di Sanità—V Programma Nazionale di Ricerca sull'AIDS 2003 (grant numbers 30F.19 and 40F.78), and Italian MIUR (PRIN 2004) for financial support.

Keywords: AIDS · antiviral agents · arylthiopyrroles · HIV · NNRTI

[1] A. Mocroft, S. Vella, T. L. Benfield, A. Chiesi, V. Miller, P. Gargalianos, A. d'Arminio-Monforte, I. Yust, J. N. Bruun, A. N. Phillips, J. D. Lundgren, *Lancet* **1998**, *352*, 1725 – 1730.

 © 2006 Wiley-VCH Verlag GmbH & Co. KGaA, Weinheim

[2] S. Vella, L. Palmisano, *Antiviral Res.* **2000**, *45*, 1 – 7.
[3] G. Barbaro, A. Scozzafava, A. Mastrolorenzo, C. T. Supuran, *Curr. Pharm. Des.* **2005**, *11*, 1805 – 1843.
[4] H. Jonckheere, J. Anné, E. De Clercq, *Med. Res. Rev.* **2000**, *20*, 129 – 154.
[5] J. P. Vacca, J. H. Condra, *Drug Discovery Today* **1997**, *2*, 261 – 272.
[6] J. M. Kilby, S. Hopkins, T. M. Venetta, B. Dimassimo, G. A. Cloud, J. Y. Lee, L. Alldredge, E. Hunter, D. Lambert, D. Bolognesi, T. Matthews, M. R. Johnson, M. A. Nowak, G. M. Shaw, M. S. Saag, *Nat. Med.* **1998**, *4*, 1302 – 1307.
[7] E. De Clercq, *Antiviral Res.* **1998**, *38*, 153 – 179.
[8] R. A. Koup, V. J. Merluzzi, K. D. Hargrave, J. Adams, K. Grozinger, R. J. Eckner, J. L. Sullivan, *J. Infect. Dis.* **1991**, *163*, 966 – 970.
[9] W. W. Freimuth, *Adv. Exp. Med. Biol.* **1996**, *394*, 279 – 289.
[10] S. D. Young, S. F. Britcher, L. O. Tran, L. S. Payne, W. C. Lumma, T. A. Lyle, J. R. Huff, P. S. Anderson, D. B. Olsen, S. S. Carroll, D. J. Pettibone, J. A. O'Brien, R. G. Ball, S. K. Balani, J. H. Lin, I.-W. Chen, W. A. Schleif, V. V. Sardana, W. J. Long, V. W. Byrnes, E. A. Emini, *Antimicrob. Agents Chemother.* **1995**, *39*, 2602 – 2605.
[11] D. M. Himmel, K. Das, A. D. Clark, S. H. Hughes, A. Benjahad, S. Oumouch, J. Guillemont, S. Coupa, A. Poncelet, I. Csoka, C. Meyer, K. Andries, C. H. Nguyen, D. S. Grierson, E. Arnold, *J. Med. Chem.* **2005**, *48*, 7582 – 7591.
[12] R. Esnouf, J. Ren, C. Ross, Y. Jones, D. Stammers, D. Stuart, *Nat. Struct. Biol.* **1995**, *2*, 303 – 308.
[13] J. Ren, D. K. Stammers, *Trends Pharmacol. Sci.* **2005**, *26*, 4 – 7.
[14] E. De Clercq, *Chem. Biodiversity* **2004**, *1*, 44 – 64.
[15] T. Fujiwara, A. Sato, M. El-Farrash, S. Miki, K. Abe, Y. Isaka, M. Kodama, Y. Wu, L. B. Chen, H. Harada, H. Sugimoto, M. Hatanaka, Y. Hinuma, *Antimicrob. Agents Chemother.* **1998**, *42*, 1340 – 1345.
[16] T. Fujiwara, A. Sato, A. K. Patrick, K. E. Potts, *Int. Antiviral News* **1999**, *7*, 18 – 20.
[17] J. Ren, C. Nichols, L. E. Bird, T. Fujiwara, H. Sugimoto, D. I. Stuart, D. K. Stammers, *J. Biol. Chem.* **2000**, *275*, 14316 – 14320.
[18] R. Di Santo, R. Costi, M. Artico, R. Ragno, S. Massa, M. La Colla, R. Loddo, P. La Colla, A. Pani, *Med. Chem. Res.* **2002**, *12*, 153 – 167.
[19] R. Di Santo, R. Costi, M. Artico, G. Miele, A. Lavecchia, E. Novellino, A. Bergamini, R. Cancio, G. Maga, *ChemMedChem* **2006**, *1*, 1367 – 1378.
[20] C. G. Kruse, A. C. V. Janse, V. Dert, A. Van der Gen, *J. Org. Chem.* **1979**, *44*, 2916 – 2920.
[21] X. Wang, S. Z. Stankovich, R. A. Widenhoefer, *Organometallics* **2002**, *21*, 901 – 905.
[22] G. Buechi, S. H. Feairheller, *J. Org. Chem.* **1969**, *34*, 609 – 612.
[23] R. Itooka, Y. Iguchi, N. Miyaura, *J. Org. Chem.* **2003**, *68*, 6000 – 6004.
[24] A. Minatti, K. H. Doetz, *Synlett* **2004**, *9*, 1634 – 1636.
[25] GOLD 2.2, CCDC Software Limited, Cambridge, UK, **2004**.
[26] G. Jones, P. Willett, R. C. Glen, A. R. Leach, R. Taylor, *J. Mol. Biol.* **1997**, *267*, 727 – 748.
[27] G. Jones, P. Willett, R. C. Glen, *J. Mol. Biol.* **1995**, *245*, 43 – 53.
[28] C. Bissantz, G. Folkers, D. Rognan, *J. Med. Chem.* **2000**, *43*, 4759 – 4767.
[29] G. Schneider, H. Bohm, *Drug Discovery Today* **2002**, *7*, 64 – 70.
[30] M. B. Smith, M. L. Lamb, J. Tirado-Rives, W. L. Jorgensen, C. J. Michejda, S. K. Ruby, R. H. Smith, Jr., *Protein Eng.* **2000**, *13*, 413 – 421.
[31] D. Wang, R. C. Rizzo, J. Tirado-Rives, W. L. Jorgensen, *Bioorg. Med. Chem. Lett.* **2001**, *11*, 2799 – 2802.
[32] R. Pauwels, J. Balzarini, M. Baba, R. Snoeck, D. Schols, P. Herdewijn, J. Desmyter, E. De Clercq, *J. Virol. Methods* **1988**, *20*, 309 – 321.
[33] M. Botta, M. Artico, S. Massa, A. Gambacorta, M. E. Marongiu, A. Pani, P. La Colla, *Eur. J. Med. Chem.* **1992**, *27*, 251 – 257.
[34] J. G. Vinter, A. Davis, M. R. Saunders, *J. Comput.-Aided Mol. Des.* **1987**, *1*, 31 – 51.
[35] A. T. Hagler, S. Lifson, P. Dauber, *J. Am. Chem. Soc.* **1979**, *101*, 5122 – 5130.
[36] "The PyMOL Molecular Graphics System": W. L. DeLano, **2002** http://pymol.sourceforge.net/.

Received: May 17, 2006
Revised: August 9, 2006
Published online on November 7, 2006

 © 2006 Wiley-VCH Verlag GmbH & Co. KGaA, Weinheim